

RECENT X-RAY MEASUREMENTS OF THE ACCRETION-POWERED PULSAR 4U 1907+09

J. J. M. IN 'T ZAND

Space Research Organization Netherlands, Sorbonnelaan 2, 3584 CA Utrecht, Netherlands; jeanz@sron.ruu.nl

A. BAYKAL

Physics Department, Middle East Technical University, Ankara 06531, Turkey; altan@astroa.physics.metu.edu.tr

T. E. STROHMAYER¹

NASA Goddard Space Flight Center, Laboratory for High-Energy Astronomy, Code 662, Greenbelt, MD 20771; stroh@lheamail.gsfc.nasa.gov

Received 1997 May 30; accepted 1997 October 24

ABSTRACT

X-ray observations of the accreting X-ray pulsar 4U 1907+09 obtained during 1996 February with the Proportional Counter Array onboard the *Rossi X-Ray Timing Explorer (RXTE)* have made possible the first measurement of the intrinsic pulse period (P_{pulse}) since 1984: $P_{\text{pulse}} = 440.341^{+0.012}_{-0.017}$ s. 4U 1907+09 is in a binary system with a blue supergiant. The orbital parameters have been solved, which enables us to correct a measurement of P_{pulse} obtained in 1990 with *Ginga* for orbital delay effects. Thus, three spin-down rates can be extracted from four pulse periods obtained in 1983, 1984, 1990, and 1996. These are equal to within 8% to a value of $\dot{P}_{\text{pulse}} = +0.225$ s yr⁻¹. This suggests that the pulsar has perhaps been in a monotonous spin-down mode since its discovery in 1983. Furthermore, the *RXTE* observations showed transient ~ 18 s oscillations during a flare that lasted about 1 hr. These oscillations could be interpreted as Keplerian motion of an accretion disk near the magnetospheric radius. This, and the notion that the corotation radius is much larger than any conceivable value for the magnetospheric radius (because of the long spin period), renders it unlikely that this pulsar spins near equilibrium, as is suspected for other slowing accreting X-ray pulsars. We suggest as an alternative that the frequent occurrence of a retrograde transient accretion disk may be consistently slowing the pulsar down. Further observations of flares could provide more evidence of this.

Subject headings: accretion, accretion disks — binaries: general — pulsars: individual (4U 1907+09) — stars: neutron — X-rays: stars

1. INTRODUCTION

4U 1907+09 is an X-ray pulsar powered by accretion of wind material from a blue supergiant companion star. It was discovered as an X-ray source by Giacconi et al. (1971) and has been studied using instruments on *Ariel V* (Marshall & Ricketts 1980, hereafter MR80), *Tenma* (Makishima et al. 1984, hereafter M84), *EXOSAT* (Cook & Page 1987, hereafter CP87), and *Ginga* (Makishima & Mihara 1992; Mihara 1995). MR80 first determined the orbital period of the binary at 8.38 days through an analysis of data taken over the course of 5 yr (between 1974 and 1980) from a survey instrument on *Ariel V*, with a net observation time of about 6 months. A folded light curve of these data shows a pronounced primary flare and a dimmer and irregular secondary flare. M84 observed 4U 1907+09 with *Tenma* in 1983 and discovered the pulsar, with a pulse period of 437.5 s. Through a good time coverage of the binary orbit, they were also able to confirm the occurrence of two phase-locked flares. The secondary flare in the *Tenma* data appears to be as bright as the primary flare. CP87 discuss *EXOSAT* data with a small though reasonably uniform coverage of the orbit. They also find evidence for phase-locked primary and secondary flares. By combining *Tenma* and *EXOSAT* data, they were able to determine the binary orbit most accurately, and found an eccentricity of $0.16^{+0.14}_{-0.11}$. A measurement of the pulse period revealed an average spin-down rate of $+0.23$ s yr⁻¹ since the *Tenma* measurement 270 days earlier. 4U 1907+09 was observed

with *Ginga* in 1990. Makishima & Mihara (1992) report a cyclotron feature at 21 keV found during these observations. Mihara (1995) measured the pulse period using the *Ginga* data; without correcting for the binary orbit, its value was determined to be 439.47 s. Sadeh & Livio (1982), using data from the *HEAO 1 A-1* instrument, report the occurrence of 15 ms oscillations during 4 out of 20 scans of the source, each lasting about 10 s. The oscillation period was seen to change during each scan.

In 1996 February, 4U 1907+09 was observed with the narrow-field instruments on the *Rossi X-Ray Timing Explorer (RXTE)*. A previous paper (in 't Zand, Strohmayer, & Baykal 1997, hereafter ISB97) reported a frequent occurrence of complete dips in the pulsar signal with durations of a few minutes to 1.5 hr found in these data. In the current paper, we report on the same data, but concentrate on the variability on timescales shorter than or equal to the pulse period. We discuss the pulse period and its history since 1983 and present evidence for the occurrence of transient oscillations. These timing diagnostics make it possible to address interesting questions about the presence of an accretion disk and the angular momentum transfer in the binary. We also briefly discuss the general spectral trend as a function of pulse phase.

2. OBSERVATIONS

RXTE-PCA (Zhang et al. 1993) consists of five identical proportional counters coaligned to the same point in the sky. Collimators limit the field of view to 1 square degree. The total geometric collecting area is approximately 6250 cm², and the effective sensitive photon energy range is 2–60

¹ Universities Space Research Association research scientist.

TABLE 1
RXTE OBSERVATION LOG OF 4U 1907+09

	OBSERVATION RUN			
	1	2	3	4
Date (U.T. 1996 Feb)	17.73–18.15	19.67–20.10	21.60–22.08	23.02–23.42
Orbital Phase ^a	0.55–0.60	0.78–0.84	0.01–0.07	0.18–0.23
Orbital Phase ^b	0.85–0.90	0.08–0.14	0.31–0.37	0.48–0.53
Exposure Time (s)	19442	19911	20261	19775
Time Span (s)	36093	37601	41658	33457

^a Based on the epoch of maximum distance between the pulsar and solar system barycenter.

^b Based on the epoch of periastron.

keV. The satellite is in a low Earth orbit, so long observations may be broken up by Earth occultations and passes through the South Atlantic Anomaly.

RXTE-PCA observed 4U 1907+09 during four observation runs, totalling 79.4 ks, which are detailed in Table 1. The mode of data collection for the four observation runs was event data with 64 energy channels resolution over the full bandpass and a time resolution of 16 μ s. No detector identification bits were telemetered. At the time of the observations, the onboard gain correction algorithm was temporarily turned off (Jahoda et al. 1996). The gains of the 5 PCA detectors are slightly different. Whenever we quote intensities in a certain energy range, we refer to the energy range consistent with the channel setting of detector PCU0. We note that the gains of the other detectors deviate by less than 0.1 keV at the low end to at most 2 keV at the high end of the range.

There are a number of known contributors to the X-ray background in our measurements: the cosmic diffuse background, the diffuse Galactic ridge emission, and the supernova remnant W49B. The latter two have not been accurately imaged yet in our bandpass. This forces us to employ a simplified background subtraction procedure, which has been detailed in ISB97: the X-ray background is defined as the residual emission found during dip times when there is no apparent pulsed emission. Using this background implies two assumptions: that if there is residual emission from 4U 1907+09 we disregard it and assume it is constant, and that there is no other variable source in the background. This second assumption seems reasonable, given the mentioned contributors, and certainly on the timescale of the observations. With regards to residual emission from 4U 1907+09, we can only note that estimates of the different contributions are prone to systematic errors, but we suggest that residual emission is at a level that is less than 2% of the average 4U 1907+09 intensity in the 2–15 keV band (ISB97).

3. THE X-RAY LIGHT CURVE

Figure 1 shows the time history of the raw count rate of the *RXTE*-PCA observations on 4U 1907+09. Apart from the dips, the pulsar signal with a period of about 440 s is obvious. The pulse profile is highly variable. It can change from pulse to pulse or even within one pulse. The time history shows a flare at Feb. 23.07, when the net 2–15 keV intensity rises by an order of magnitude to about 0.1 crab. Given the newly determined orbital period (see § 4), this flare occurs 543.99 ± 0.04 orbital periods after the secondary and 544.44 ± 0.04 orbital periods after the primary flare

as observed with *Tenma* in 1983 August and September (M84), the most recent timing reports of flares. The identification of the flare on Feb. 23.07 with the secondary flare seems unambiguous, and so we confirm the recurrence of a phase-locked secondary flare. It is interesting to note that the orbital phase of the flare (see Table 1) places it near to the time of apastron of the binary. The intensity of the flare (in 2–30 keV) is about twice as high as the one measured with *Tenma* (M84). This is not unexpected. The secondary flare has been seen to vary from insignificant to as bright as the primary flare (MR80). We note that the observed flare may actually be only part of a more extended secondary flare that could have been missed because of the sparsity of the *RXTE* coverage. The *Tenma* observation of the secondary flare suggests that the flare may last 0.3 days; the associated uncertainty in the epoch has been included in the uncertainty mentioned above of the number of orbital periods since the flares observed by *Tenma*.

4. TIMING ANALYSIS OF THE PULSE SIGNAL

An initial estimate of the pulse period was obtained by folding the 2–15 keV time history into a number of statistically independent trial periods (Leahy et al. 1983) in the range of 430–450 s. Only data outside the intensity dips were used, and photon arrival times were corrected into those for the solar system barycenter. The highest χ^2 value was found for a period of 440.4 s (see Fig. 2).

In order to accurately determine the pulse period as well as the binary orbit, a set of 19 pulse arrival times was generated, one pulse arrival time for each *RXTE* orbit when 4U 1907+09 is not in a dip. This was done by folding the time history data into one average pulse for each *RXTE* orbit, folding *all* time history data into one master pulse, and cross-correlating the master pulse with each of the 19 average pulses to find the pulse arrival times. Average profiles rather than individual pulses were used to minimize systematic effects arising from the sometimes strong changes in the profile from pulse to pulse, which are supposedly due to variability in the accretion rate (ISB97).

As an alternative, to control the pulse profile variability we have used the method of pulse wave filtering, as proposed by Deeter & Boynton (1985; see also Boynton et al. 1986). In this method, pulse profiles are expressed in terms of harmonic series and cross-correlated with the average pulse profile (the “master pulse”). The maximum value of the cross-correlation is analytically well defined and does not depend on the phase binning of the pulses. The short-term sharp fluctuations of pulses are naturally filtered by a cutoff of higher harmonics. The pulse arrival times obtained

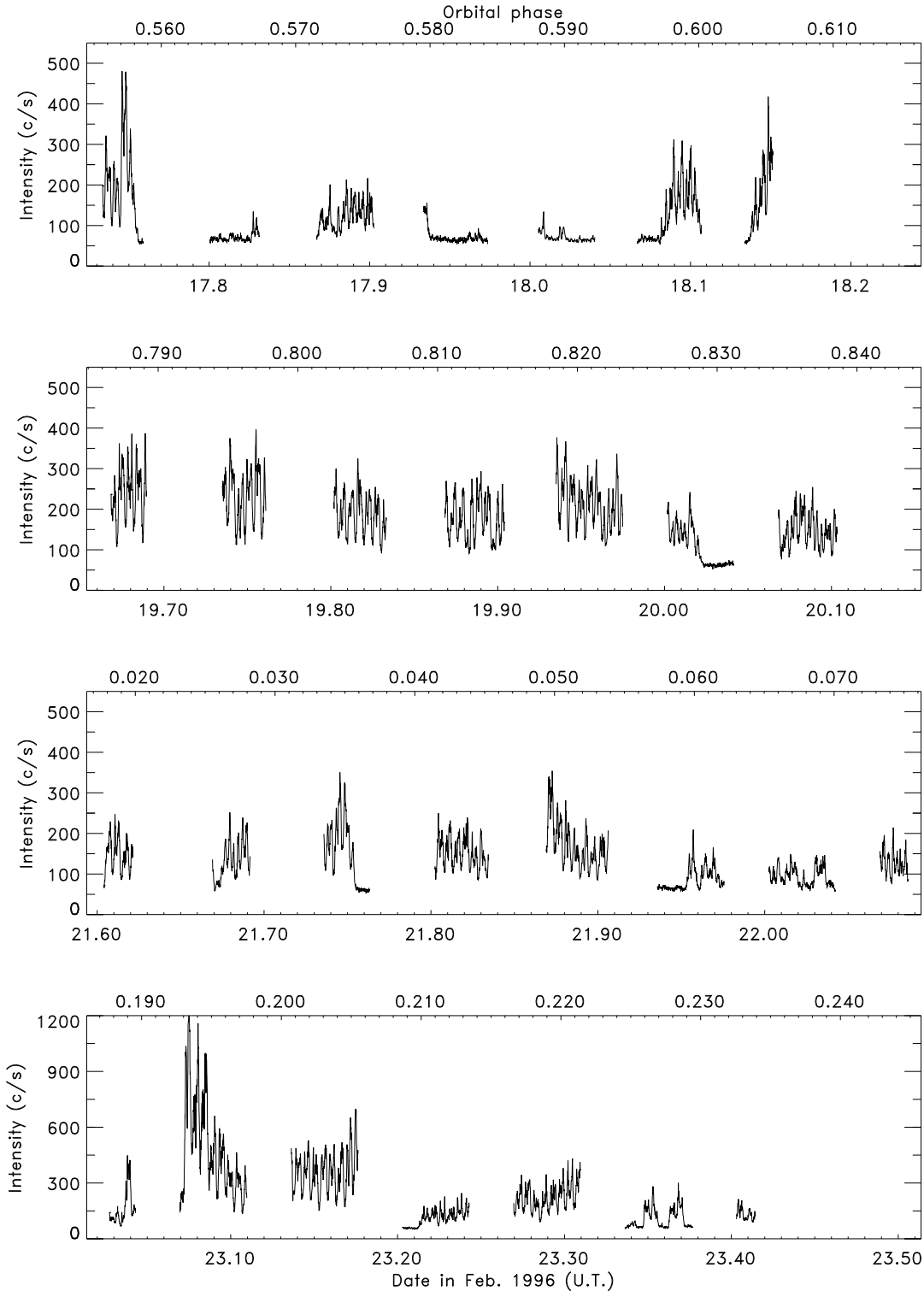


FIG. 1.—Time histories of the raw *RXTE*-PCA 2–15 keV intensity of 4U 1907+09, bin time 32 s. Orbital phases are with respect to the epoch of maximum distance between the pulsar and the solar system barycenter.

with this method gave statistically the same results as those obtained with the method detailed above.

In order to increase the accuracy of the orbital solution (in particular the orbital period), the pulse arrival times were combined with the pulse delay time data from *Tenma* observations, as published graphically by M84.

We modeled the data with an eccentric orbit using parameters that have not changed since the *Tenma* observations in 1983 September and a pulse period that is constant throughout our *RXTE* observations. We determined these parameters by testing the model against the data using Pearson's χ^2 test on a grid of parameter values suffi-

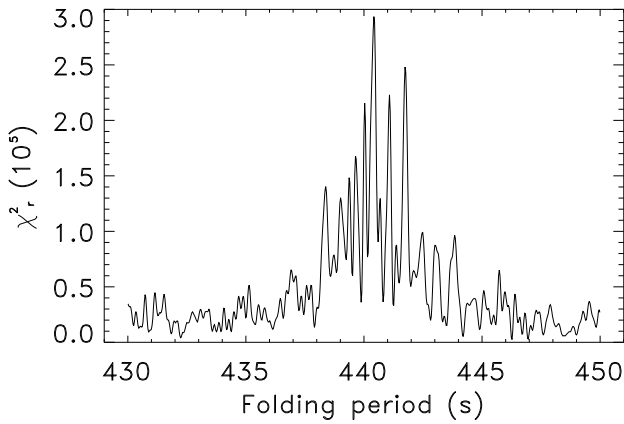


FIG. 2.—Periodogram of the 2–15 keV time history data after correction to solar system barycenter, but before correction to binary system barycenter.

ciently sampled to detect significant changes in χ^2 and with a range that sufficiently encloses the allowed parameter values. The parameters are the pulse period P_{pulse} at the time of the *RXTE* observations, the orbital period P_{orb} , the epoch $T_{\pi/2}$ of mean longitude 90° (i.e., one-quarter of the orbital period after the time of ascending node, when the neutron star crosses the sky tangent plane through the barycenter moving away from the observer), the longitude of periastron ω (i.e., with respect to the ascending node), the eccentricity e , and the length of the projected semimajor axis $a_x \sin i/c$. The grid ranges and sample frequencies were found iteratively, going from a rough to a sufficiently fine grid. We choose this grid search method in order to be able to determine the uncertainty of the solution with any arbitrary confidence level. The χ^2 values were calculated in the pulse delay time domain. This enables us to include *Tenma* data that have not been published in the pulse arrival time domain; however, it also precludes the determination of P_{pulse} during the *Tenma* observations. We fixed the error in the pulse delay times at 8 s. This value was suggested by the uncertainty of the harmonics in the pulse wave filtering analysis of the *RXTE* data, and it is also the value M84 adopted for the *Tenma* data.

The results of modeling the timing data are presented in Table 2. The quoted error intervals are projections of the 68% confidence level region onto each of the six parameter axes. Since some parameters are very dependent, the actual solution is confined within a much smaller space than that of the six-dimensional cube dictated by the quoted errors. The errors are, therefore, conservative. For the purpose of easy comparison with orbital solutions by others, we have also included the single-parameter 1σ errors in Table 2.

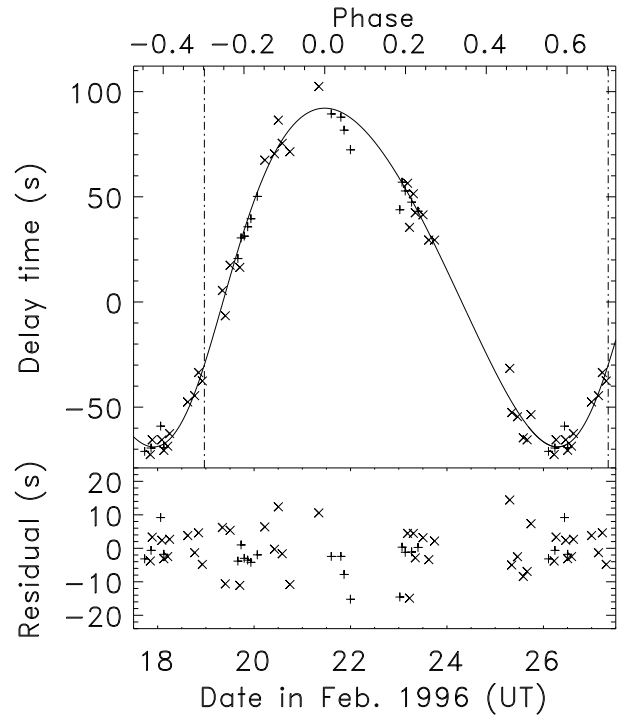


FIG. 3.—Delay time vs. time for the *RXTE* measurements (plus signs) and *Tenma* measurements folded into the *RXTE* time of observation (crosses). The phases indicated at the top are with respect to the time of maximum distance between the pulsar and the solar barycenter. Solid line shows the model for the eccentric orbit specified in Table 2. Vertical dashed lines show the inferred times of periastron. All data points are repeated modulo P_{orb} . The rms of the residuals is 6.6 s.

Figure 3 presents a plot of the orbital model against the data in terms of delay times with respect to the binary barycenter.

The orbital solution provides a way to correct the pulse period determined with *Ginga* in 1990 (Mihara 1995) for the orbital motion of the neutron star in the binary system. The *Ginga* observations were performed for a duration of 14 hr (this is 0.07 in phase) at a mean time of MJD 48156.60. This is 0.10 orbital periods after the epoch of ascending node, where the orbital Doppler shift is +0.28 s per pulse period, with an uncertainty of about 0.01 s per pulse period. Therefore, the corrected pulse period is 439.19 s.

We find a pulse period at the time of the *RXTE* observations of $440.341^{+0.012}_{-0.017}$ s. This completes a total of four measurements of the pulse period and three measurements of the pulse period derivative since 1983. These values, tabulated in Table 3, suggest an interesting finding: the pulsar appears to be spinning down with a close to constant deriv-

TABLE 2
BINARY ORBIT AND PULSE PERIOD OF 4U 1907+09 FROM 1983 *Tenma* AND 1996 *RXTE*-PCA MEASUREMENTS

Parameter	Symbol	Value	68% Confidence Region	Single-parameter 1σ Error
Orbital period	P_{orb}	8.3753 days	+0.0003 -0.0002	0.0001
Eccentricity	e	0.28	+0.10 -0.14	0.04
Orbital epoch	$T_{\pi/2}$	MJD 50134.76	+0.16 -0.20	0.06
Longitude of periastron	ω	330°	+20 -20	7
Projected semimajor axis length	$a_x \sin i/c$	83 lt-s	+4 -4	2
Pulse period	P_{pulse}	440.341 s	+0.012 -0.017	0.006

TABLE 3
HISTORY OF P_{pulse} MEASUREMENTS FOR 4U 1907+09

Date	Mean Time (MJD)	Satellite	Reference	P_{pulse} (s)	Derivative ^a (s yr ⁻¹)
1983 Aug/Sep	45576	<i>Tenma</i>	M84	437.483 ± 0.004	
1984 May/June	45850	<i>EXOSAT</i>	CP87	437.649 ± 0.019	0.22 ± 0.03
1990 Sep	48156.6	<i>Ginga</i>	Mihara 1995	439.19 ± 0.02^b	0.244 ± 0.005
1996 Feb	50134	<i>RXTE</i>	This paper	440.341 ± 0.014	0.212 ± 0.004

^a Pulse period derivative is calculated from the difference in P_{pulse} with respect to the previous observation in this table.

^b This value was corrected for delays from binary motion in the present work. The uncertainty is an estimate.

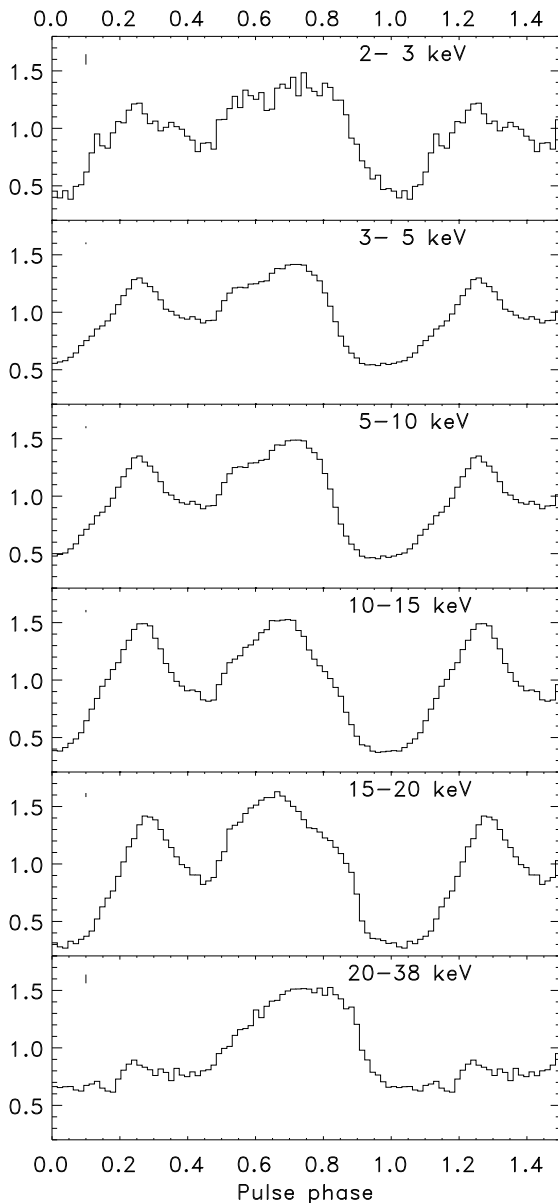


FIG. 4.—Background-subtracted light curve folded with the pulse period for six bandpasses between 2 and 38 keV. The bandpasses are indicated in each panel, and the statistical 1σ error is shown in the upper left corner (from top to bottom, these errors are 0.045, 0.007, 0.009, 0.010, 0.018, and 0.038). The phase offset is arbitrary. The unit of intensity is the average intensity per bandpass. Only data for “quiet” periods, when the source is neither dipping nor flaring above 500 c s^{-1} , is used. The net exposure time for these light curves is 29.6 ks out of a total of 79 ks.

ative. The three values are within 8% of a mean value of $\dot{P}_{\text{pulse}} = +0.225\text{ s yr}^{-1}$.

As mentioned above, we assume that over the course of 12 yr there is no noticeable change in P_{orb} , ω , and the orbit inclination angle i . For P_{orb} , we can confirm this with reasonable accuracy because the value we find is, within error margins, equal to what was found by CP87 between the *Tenma* and *EXOSAT* measurements (8.3745 ± 0.0042 days). For ω , the uncertainty, typically 20° , is simply too large for us to be able to measure likely values for the change (for a detailed analysis of apsidal advance in the similar system Vela X-1, see Deeter et al. 1987). The same argument holds for the sensitivity to measuring changes in i .

The photon arrival times were folded with the pulse period after correction for the Earth’s motion around the Sun, *RXTE*’s motion around the Earth, and the binary motion of the pulsar. The resulting pulse profile is presented in Figure 4 for six photon energy bands up to 38 keV. Above this energy, no pulsed emission was detected, as revealed by a Fourier analysis (Fig. 5). The pulse profiles are expressed in units of average 4U 1907+09 intensity per band. The background in each band was determined as discussed in ISB97 (see § 2). The pulse profile consists of two peaks with a deep and a shallow minimum in between that are close to 0.5 in pulse phase apart. It appears similar to that observed more than a decade before with *Tenma* and *EXOSAT* in similar energy bands (M84; CP87). It is rather insensitive to energy between 2 and 20 keV, although subtle dependencies are noticeable, particularly in the second peak. There is a dramatic change of the pulse profile at

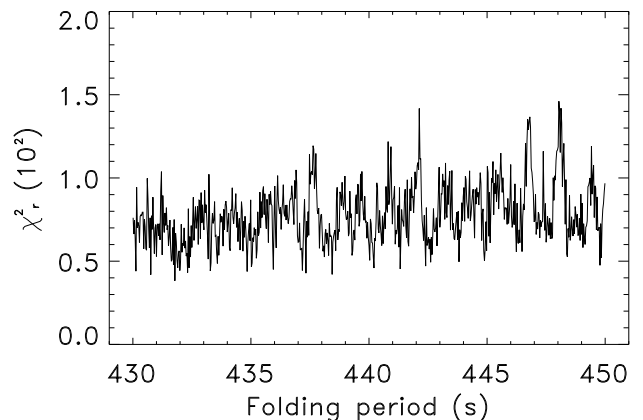


FIG. 5.—Periodogram of the $>40\text{ keV}$ time history data after correction to solar barycenter but before correction to binary barycenter.

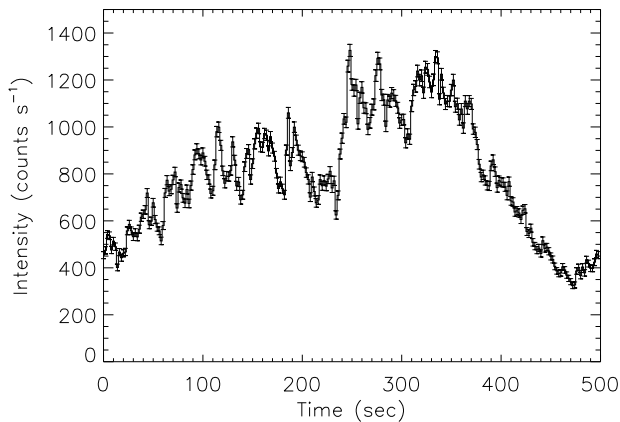


FIG. 6.—Expanded view of the observed X-ray time profile during the secondary flare in the full PCA bandpass. Time is measured from 1996 February 23, 01:56:33 UTC.

around 20 keV. Basically, the first pulse disappears above that energy and the shape of the second one changes. The modulation depth is roughly the same in all bands. The energy dependency of the pulse profile appears to be similar to that observed in Cen X-3 with *Ginga* (Nagase et al. 1992).

5. TRANSIENT 18 s OSCILLATIONS

Visual inspection of the X-ray light curve on second time-scales during the flare at Feb. 23.07 suggests that there is a variety of non-Poissonian variability present during the flare. For example, Figure 6 shows the light curve of a 500 s interval near the peak of the flare. Fluctuations in the count rate as large as several hundred counts s^{-1} are obvious in this light curve. To further quantify this short-timescale variability (i.e., shorter than a pulse period), we computed Fourier power spectra for the time intervals encompassing the flare. The power spectrum of a 1024 s interval beginning 300 s prior to that shown in Figure 6 is displayed in Figure 7. There are a number of conspicuous peaks in this power spectrum in the range of 0.02–0.06 Hz. There is also clearly a broadband noise component increasing toward lower frequencies, as the mean power is significantly above 2 (the mean expected for purely Poisson fluctuations) extending above 0.2 Hz. One of the most prominent peaks is at 0.055 Hz, or a period of 18.2 s. These 18 s oscillations can actually be seen with the eye in Figure 6. To investigate further, we

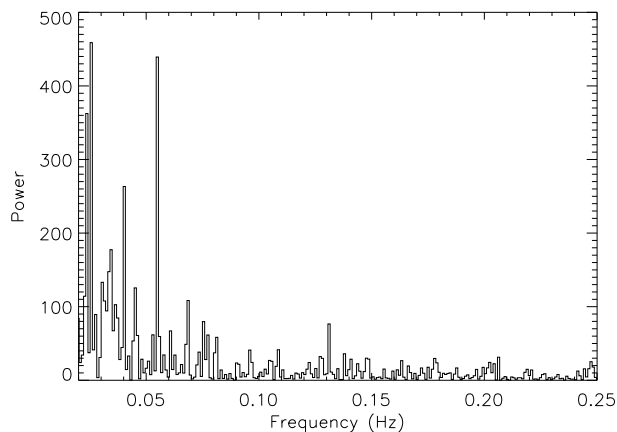


FIG. 7.—Power spectrum of a 1024 s piece of the light curve, starting 300 s before the start time indicated in Fig. 6.

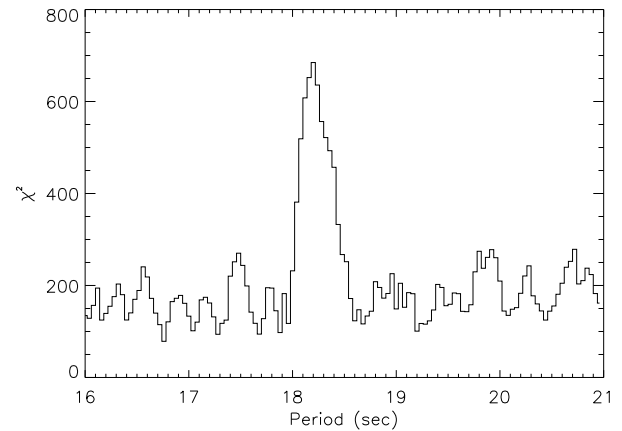


FIG. 8.—Periodogram near 18 s for the flare data

performed an epoch-folding period search in the vicinity of 18 s. The results are shown in Figure 8, and there is an obvious peak centered at 18.2 s. To determine the average amplitude of the oscillations, we folded the 1024 s of data into the best-fit period of 18.2 s. We then fitted a model that includes a constant count rate and a sinusoid to the folded data. Figure 9 shows the resulting background-subtracted light curve and the best-fit sinusoidal model. The χ^2 per degree of freedom is formally a bit high, 1.8, but for estimating the amplitude of the oscillation the sinusoidal fit is sufficient. From this analysis we obtain an average oscillation amplitude of $4.4 \pm 0.3\%$, where the amplitude is defined as the ratio of the sinusoidal to the constant count rate components. We also investigated the dependence on photon energy of both the pulsation amplitude and the pulse profile, but found no significant energy dependence.

The 18 s oscillations are not persistent; rather, they are confined to an approximately 1000 s interval centered near the peak of the flare. To investigate the transient nature of the 18 s oscillation, we computed a dynamic power spectrum by calculating power spectra from 500 s intervals with a new interval beginning every 50 s. The resulting power spectra are not independent, since the data segments overlap, but this method identifies the range of times for which the 18 s oscillations are present. The resulting dynamic spectrum is shown in the top panel of Figure 10.

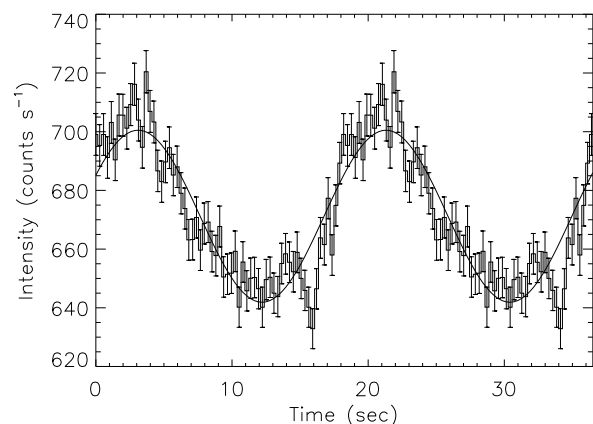


FIG. 9.—Background-subtracted light curve folded with a period of 18.2 s and a sinusoidal fit to the data.

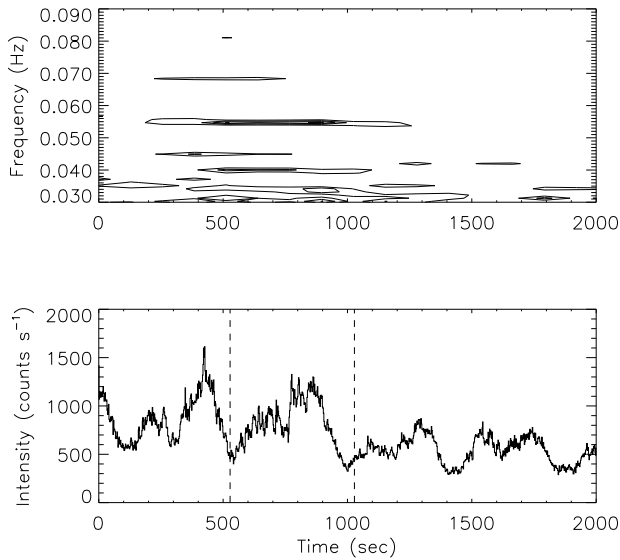


FIG. 10.—*Top panel*: Contour map of the dynamic power spectrum. *Bottom panel*: Accompanying light curve. Vertical dashed lines show the time frame of Fig. 6.

The 0.055 Hz oscillations are clearly present from about 200–1200 s, and this is the only epoch in which we detected such oscillations. During the period when the oscillations are present, there is no strong evidence for significant frequency drift; this gives a lower limit to the Q -value for the oscillation of $Q = (1000 \text{ s}/18.2 \text{ s}) = 55.6$ (Q being the so-called quality factor that measures the number of oscillations that will pass before a substantial fraction of the energy of the oscillator is dissipated; Q is inversely proportional to the bandwidth or spectral purity of the oscillation).

To investigate the nature of the broadband noise, we computed an average fast Fourier transform power spectrum from two successive orbits during the flare, for a total of 6250 s of data. The resulting average power spectrum is shown in Figure 11. We fitted a power-law model, $P = K\nu^{-\alpha}$, to 51 frequency bins in the 0.02–4 Hz frequency range. We did not fit below 0.02 Hz because there the power spectrum is dominated by the pulsed signal and its harmonics. The power-law model with $K = 0.41 \pm 0.07$ and $\alpha = 1.36 \pm 0.06$ provides an acceptable fit, with a $\chi^2/\text{dof} = 39/49 \approx 0.8$. The integrated power from 0.02 to 4 Hz corresponds to an amplitude (rms) of about 8.2%.

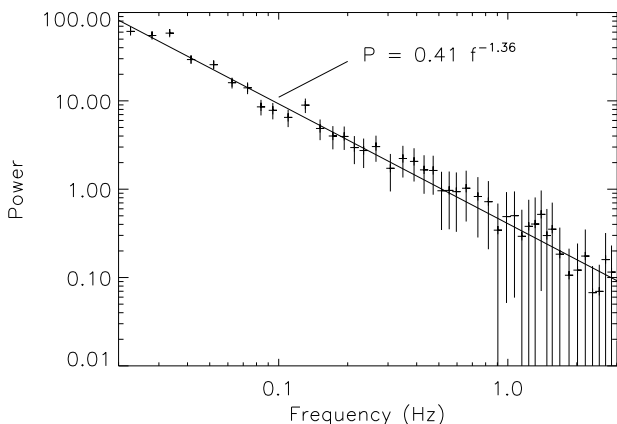


FIG. 11.—Power spectrum of the broadband noise

We note that we have searched for pulsations at higher frequencies and failed to find any. No pulsations similar to those reported by Sadeh & Livio (1982) are present at a period of around 15.3 ms. During the flare, we find an upper limit for the amplitude of 0.5%, as compared to the amplitude of 12% at which pulsations were seen by Sadeh & Livio.

6. DISCUSSION

Quasi-periodic oscillations (QPO) with frequencies in the 10–200 mHz range have been observed from seven other X-ray pulsars. Among these, A0535 + 26 (Finger, Wilson, & Harmon 1996), X1626 – 67 (Shinoda et al. 1990), Cen X-3 (Takeshima et al. 1991), V0332 + 53 (Takeshima et al. 1994), X0115 + 63 (Soong & Swank 1989), and SMC X-1 (Angelini 1989) all have QPO frequencies in the 0.062–0.1 Hz regime, similar to the 0.055 Hz transient oscillation from 4U 1907 + 09 described above. The $\approx 4\%$ amplitude (rms) of the 18 s oscillation is also similar to the amplitudes of QPO from other X-ray pulsars (see Takeshima et al. 1994; Angelini, Stella, & Parmar 1989); however, QPO detected in these sources are typically broader, with Q -values on the order of a few compared to about 50 for the 18 s oscillation in 4U 1907 + 09.

To date, almost all models of QPO in X-ray pulsars postulate the existence of an accretion disk as the site of QPO production. In the case of QPO from A0535 + 26, this is supported by the observed correlation of the QPO frequency and the spin-up rate (Finger et al. 1996), strongly suggesting a transfer of angular momentum from accretion disk to neutron star. Thus, one possibility is that the 18 s oscillations reveal the presence of a transient accretion disk during the flare.

Assuming that the 18 s oscillation in 4U 1907 + 09 is related to orbital motion, via either a beat frequency model (BFM; Lamb et al. 1985; Alpar & Shaham 1985) or a Kepler frequency model (KFM; van der Klis et al. 1987), then the inferred radius of material in a putative disk is $R_d = (GM/4\pi^2\nu_{\text{QPO}}^2)^{1/3} \approx 1.2 \times 10^4 \text{ km}$ for a $1.4 M_\odot$ neutron star. This is nearly an order of magnitude smaller than the corotation radius, $R_c = 9.6 \times 10^4 \text{ km}$, for this object. We can roughly estimate the size of the neutron star magnetosphere from the expression for the Alfvén radius, assuming spherical accretion (e.g., Ghosh & Lamb 1991), as

$$R_m = 2.4 \times 10^3 (M/1.4 M_\odot)^{1/7} (B/2.5 \times 10^{12} \text{ G})^{4/7} \\ \times (R/10^6 \text{ cm})^{10/7} (L_x/3.1 \times 10^{37} \text{ ergs s}^{-1})^{-2/7} \text{ km} . \quad (1)$$

Studies of the optical counterpart, discovered by Schwartz et al. (1972), reveal that the distance to 4U 1907 + 09 is between 2.4 and 5.9 kpc (Van Kerkwijk et al. 1989). Assuming that the distance is 4 kpc, the average nonabsorbed luminosity of 4U 1907 + 09 during nondip and non-flare periods and within the studied energy range is $L_x = 1 \times 10^{36} \text{ ergs s}^{-1}$ (ISB97). During the flare, the luminosity increases to $4 \times 10^{36} \text{ ergs s}^{-1}$. For a flare X-ray luminosity of $4 \times 10^{36} \text{ ergs s}^{-1}$, a magnetic field $B = 2.5 \times 10^{12} \text{ G}$, a stellar mass of $1.4 M_\odot$, and a radius of 10 km, $R_m \approx 4300 \text{ km}$. Although this number is rather uncertain, it suggests that the disk can certainly penetrate close enough to the star to account for the 18 s oscillations as an orbital phenomenon associated with an accretion disk. Although the accretion disk interpretation seems plausible, further

observations, particularly in the vicinity of the flare, will be required to confirm it.

Long-term measurements of the behavior of the spin period for a selection of 15 accreting X-ray pulsars (AXPs) (Bildsten et al. 1997) show that three known pulsars appear to exhibit systematic spin-down evolution for at least 5 yr: GX1+4 ($P/\dot{P} \approx 90$ yr), 4U 1626–67 ($P/\dot{P} \approx 5 \times 10^3$ yr), and Vela X-1 ($P/\dot{P} \approx 6 \times 10^3$ yr). Generally, this behavior is attributed to low accretion rates that bring the magnetospheric radius R_m close to the corotation radius R_c (Ghosh & Lamb 1979a, 1979b; Wang 1987, 1995; Anzer & Börner 1980; Lovelace, Romanova, & Bisnovaty-Kogan 1995). However, for 4U 1907+09 this is an unlikely scenario, because the magnetospheric radius is hard to bring out to such a large corotation radius unless the magnetic field is of the unlikely order of 10^{14} G or the distance is on the order of 0.5 kpc, which is at least 5 times lower than studies of the optical counterpart suggest.

The putative disk supports the notion that the magnetospheric radius is substantially smaller than the corotation radius. Moreover, a transient disk can provide an alternative explanation to the observed spin-down if this disk is rotating in an opposite sense to the pulsar spin. Such a disk could provide the necessary torque to explain the spin-down rate. If all accreted mass supplies its angular momentum at a radius R_d , then the expected torque on the neutron star is $N_{\text{char}} = \eta M (GMR_d)^{1/2}$, where $\eta < 1$ is the duty cycle of the transient disk. If we assume that all the potential energy of the accreted mass liberated during the flare is transformed into radiation and that the flare luminosity is $3.2 \times 10^{35} D_{\text{kpc}}^2 \text{ ergs s}^{-1}$, then $N_{\text{char}} = 2.5 \times 10^{22} \eta D_{\text{kpc}}^2 R_d^{1/2}$. For $R_d = 1.2 \times 10^4$ km, this becomes $N_{\text{char}} = 8.6 \times 10^{32} \eta D_{\text{kpc}}^2 \text{ g cm}^2$. The observed absolute value of the torque is $N_{\text{obs}} = 2\pi I |\dot{\nu}|$, where I is the moment of inertia and $\dot{\nu} = -3.7 \times 10^{-14} \text{ Hz s}^{-1}$ (equivalent to $\dot{P} = +0.225 \text{ s yr}^{-1}$). If $I = 10^{45} \text{ g cm}^2$ (the generic value for a neutron star of radius 10 km and mass $1.4 M_{\odot}$), $N_{\text{obs}} = 2.3 \times 10^{32} \text{ g cm}^2$. If $N_{\text{obs}} = N_{\text{char}}$ and $2.4 < D_{\text{kpc}} < 5.9$, then $0.008 < \eta < 0.05$. Therefore, the putative retrograde transient accretion disk could provide the torque to spin-down the pulsar if it lasts on average on the order of a few percent of the time. We observed a duty cycle of about 1000 s out of an orbital period of 8.4 days, which is an order of magnitude too small. However, the coverage of our observations is limited, and the flare might also have a larger duty cycle averaged over many orbits. This is confirmed by *Tenma* observations, which suggest a duration of 0.3 days for one flare (M84). We conclude that the putative retrograde accretion disk could possibly supply enough negative torque to spin-down the pulsar.

The suggestion of a retrograde accretion disk being responsible for an extensive spin-down period has recently been revisited in the case of the disk-fed accreting X-ray pulsar GX1+4 by Chakrabarti et al. (1997), in pursuit of an elegant explanation for the positive correlation between luminosity and negative torque. Our need for a retrograde accretion disk in the wind-fed 4U 1907+09 is motivated by a corotation radius that is clearly much larger than the magnetospheric radius.

4U 1907+09 is in several ways similar to Vela X-1: the spin periods of both are on the order of several hundred seconds (440 s for 4U 1907+09, 283 s for Vela X-1), the orbital periods are on the order of 8 days (8.38 days for 4U 1907+09, 8.96 days for Vela X-1), and both have recently

been found to show long periods of systematic spin-down (e.g., Bildsten et al. 1997 for Vela X-1). The occasional spin-down periods in Vela X-1 have previously been attributed to the presence of a disk with an inner edge close to the corotation radius (Nagase 1989), with the note that this implies relatively large magnetic fields (surface fields on the order of 10^{13} G). We suggest that since this reasoning goes awry in the case of 4U 1907+09, this conclusion may be invalid for Vela X-1 as well. One important difference between the two systems is that Vela X-1 shows much more spectral variability and pronounced iron lines. This may be the result of a difference in angle of sight of the binary orbit, a difference in the spatial distribution of the wind from the companion star, and/or a somewhat different eccentricity.

Compared to some other AXPs, there is moderate spectral variability within the pulse profile. Basically, the pulse profile shows two peaks below and one peak above ~ 20 keV. This is somewhat similar to what has been observed from the much more luminous disk-fed AXP Cen X-3, and it may be associated with two magnetic poles that either have different physical circumstances or are viewed at different angles by the observer. A modeling of the pulse profile, similar to studies performed by Bulik et al. (1995), but beyond the scope of this paper, may provide more definite conclusions.

Since its discovery by MR80, the occurrence of two flares per orbit has been difficult to reconcile with the identification of the companion as a supergiant high-mass star (e.g., Van Kerkwijk et al. 1989; ISB97). It has been thought that these stars do not have a circumstellar disk, as is presumed for Be stars. However, recently evidence has been mounting that in hot supergiants in the upper part of the H-R diagram, axial symmetry may play an important role (e.g., Zickgraf et al. 1996 and references therein). Also recently, another wind-fed AXP with a supergiant companion, GX 301–2, has been shown to consistently display two flares per orbit (Pravdo et al. 1995; Chichkov et al. 1995; Koh et al. 1997). This again supports the notion that the wind from the companion is not isotropic but that the mass flux is enhanced along the equatorial plane. The two flares may then be caused by the neutron star traversing this plane twice per orbit in a sufficiently inclined orbit. It is interesting to note in this context that GX 301–2 (Sato et al. 1986) and 4U 1907+09 have the highest eccentricity of the group of supergiant high-mass X-ray binaries; perhaps these systems are not yet in a tidal equilibrium. Perhaps even the spin orientation of the neutron star differs by more than 90° from the orbital motion orientation. However, at the moment this is mere speculation.

7. CONCLUSION

We have determined the pulse period of 4U 1907+09 at a recent epoch and find that the pulsar has spun down on average by 0.225 s yr^{-1} since its discovery in 1983. Three measurements of the spin-down rates during an intermediate time interval spanning between 1 and 6 yr are consistent to within 8% of this value. This suggests a remarkably monotonous spin-down trend during about 12 yr. Furthermore, we find the occurrence of 18 s oscillations for 10^3 s of a flare with a high Q value, hinting at an accretion disk. The indication that the magnetospheric radius is much smaller than the corotation radius, the observed long and constant spin-down trend, and the occurrence of transient oscillations suggest that possibly a recurrent transient accretion

disk counterrotates the neutron star and slows the pulsar down through a transfer of angular momentum. This suggestion needs to be confirmed at least by detailed multiple observations of the flares that are almost certainly recurring every orbital period.

We thank the members of the *RXTE* Guest Observer Facility for their help in the data reduction and the anonymous referee for useful suggestions.

J. Z. and A. B. acknowledge support under the research associateship program of the U. S. National Research Council during their stay at the NASA Goddard Space Flight Center, where part of the research presented in this paper was performed. T. S. acknowledges the support of the HEAP program of the Universities Space Research Association at the NASA Goddard Space Flight Center.

REFERENCES

- Alpar, M. A., & Shaham, J. 1985, *Nature*, 316, 239
- Angelini, L. 1989, in Proc. 23d ESLAB Symp., Two Topics in X-Ray Astronomy, Vol. 1, ed. N. White (Garching: ESA), 81
- Angelini, L., Stella, L., & Parmar, A. N. 1989, *ApJ*, 346, 906
- Anzer, U., & Börner, G. 1980, *A&A*, 83, 133
- Bildsten, L., et al. 1997, *ApJS*, 113, 367
- Boynton, P. E., Deeter, J. E., Lamb, F. K., & Zylstra, G. 1986, *ApJ*, 307, 545
- Bulik, T., Riffert, H., Meszaros, P., Makishima, K., Mihara, T., & Thomas, B. 1995, *ApJ*, 444, 405
- Chakrabarty, D., et al. 1997, *ApJ*, 481, L101
- Chichkov, M. A., Sunyaev, R. A., Lapshov, I. Y., Lund, N., Brandt, S., & Castro-Tirado, A. 1995, *Pis'ma Astron. Zh.*, 21, 491
- Cook, M. C., & Page, C. G. 1987, *MNRAS*, 225, 381 (CP87)
- Deeter, J. E., & Boynton, P. E. 1985, Proc. Inuyama Workshop on Timing Analysis of X-Ray Sources, ed. S. Hayakawa & F. Nagase (Nagoya: Univ. Nagoya), 29
- Deeter, J. E., Boynton, P. E., Lamb, F. K., & Zylstra, G. 1987, *ApJ*, 314, 634
- Finger, M. H., Wilson, R. B., & Harmon, B. A. 1996, *ApJ*, 459, 288
- Ghosh, P., & Lamb, F. K. 1979a, *ApJ*, 232, 259
- . 1979b, *ApJ*, 234, 296
- . 1991, in *Neutron Stars: Theory and Observation*, ed. J. Ventura & D. Pines, NATO ASI Ser. 43 (Washington: NATO), 363
- Giacconi, R., Kellogg, E., Gorenstein, P., Gursky, H., & Tananbaum, H. 1971, *ApJ*, 165, L27
- in 't Zand, J. J. M., Strohmayer, T. E., & Baykal, A. 1997, *ApJ*, 479, L47 (ISB97)
- Jahoda, K., Swank, J. J., Giles, A. B., Stark, M. J., Strohmayer, T., & Zhang, W. 1996, *Proc. SPIE*, 2808, 59
- Koh, D. T., et al. 1997, *ApJ*, 479, 933
- Lamb, F. K., Shibasaki, N., Alpar, M. A., & Shaham, J. 1985, *Nature*, 317, 681
- Leahy, D. A., Darbro, W., Elsner, R. F., Weisskopf, M. C., Sutherland, P. G., Kahn, S., & Grindlay, J. E. 1983, *ApJ*, 266, 160
- Lovelace, R. V. E., Romanova, M. M., & Bisnovatyi-Kogan, G. S. 1995, *MNRAS*, 275, 244
- Makishima, K., Kawai, N., Koyama, K., Shibasaki, N., Nagase, F., & Nakagawa, M. 1984, *PASJ*, 36, 679 (M84)
- Makishima, K., & Mihara, T. 1992, in Proc. Yamada Conf. 28, *Frontiers of X-Ray Astronomy*, ed. Y. Tanaka & K. Koyama (Tokyo: Universal Academy), 23
- Marshall, N., & Ricketts, M. J. 1980, *MNRAS*, 193, 7P (MR80)
- Mihara, T. 1995, Ph.D. thesis, Univ. of Tokyo
- Nagase, F. 1989, *PASJ*, 41, 1
- Nagase, F., Corbet, R. H. D., Day, C. S. R., Inoue, H., Takeshima, T., Yoshida, K., & Mihara, T. 1992, *ApJ*, 396, 147
- Pravdo, S. H., Day, C. S., Angelini, L., Harmon, B. A., Yoshida, A., & Saraswat, P. 1995, *ApJ*, 454, 872
- Sadeh, D., & Livio, M. 1982, *ApJ*, 258, 770
- Sato, N., Nagase, F., Kawai, N., Kelley, R. L., Rappaport, S., & White, N. E. 1986, *ApJ*, 304, 241
- Schwartz, D. A., Bleach, R. D., Boldt, E. A., Holt, S. S., & Serlemitsos, P. J. 1972, *ApJ*, 173, L51
- Shinoda, K., et al. 1990, *PASJ*, 42, L43
- Soong, Y., & Swank, J. H. 1989, in Proc. 23d ESLAB Symp., Two Topics in X-Ray Astronomy, Vol. 1, ed. N. White (Garching: ESA), 617
- Takeshima, T., et al. 1991, *PASJ*, 43, L43
- Takeshima, T., Dotani, T., Mitsuda, K., & Nagase, F. 1994, *ApJ*, 436, 871
- van der Klis, M., Jansen, F., van Paradijs, J. P., Lewin, W. H. G., Trumper, J., & Sztajno, M. 1987, *ApJ*, 313, L19
- Van Kerkwijk, M. H., Van Oijen, J. G. J., & van den Heuvel, E. P. J. 1989, *A&A*, 209, 173
- Wang, Y. M. 1987, *A&A*, 183, 257
- . 1995, *ApJ*, 449, L153
- Zhang, W., Giles, A. B., Jahoda, K., Soong, Y., Swank, J. H., & Morgan, E. H. 1993, *Proc. SPIE*, 2006, 324
- Zickgraf, F.-J., Humphreys, R. M., Lamers, H. J. G. L. M., Smolinski, J., Wolf, B., & Stahl, O. 1996, *A&A*, 315, 510